Korean J. Chem. Eng., 35(8), 1716-1725 (2018)
DOI: 10.1007/s11814-018-0064-2

pISSN: 0256-1115
eISSN: 1975-7220

Developing homogeneous ion exchange membranes derived from sulfonated polyethersulfone/N-phthaloyl-chitosan for improved hydrophilic and controllable porosity

Zhixue Li*, Zhun Ma*,†, Yuting Xu*, Xiaomeng Wang*, Yongchao Sun*, Rong Wang*, Jian Wang, Xueli Gao***,†, and Jun Gao***

*College of Chemical and Environmental Engineering, Shandong University of Science and Technology, Qingdao 266590, P. R. China
**The Institute of Seawater Desalination and Multipurpose Utilization, SOA, Tianjin 300192, P. R. China
***Key Laboratory of Marine Chemistry Theory and Technology, Ministry of Education, College of Chemistry and Chemical Engineering, Ocean University of China, Qingdao 266100, P. R. China
(*Received 28 November 2017 • accepted 10 April 2018*)

Abstract−Ion exchange membranes (IEMs) composed of sulfonated poly (ether sulfone) (SPES) and N-phthaloyl chitosan (NPHCs) were synthesized. NPHCs was employed in membrane fabrication to improve the porosity and hydrophilicity of membranes. The effect of blend ratio of sulfonation (DS) and NPHCs content on physico-chemical characteristics of home-made membranes was investigated. The morphology of prepared membranes was investigated by Fourier transform infrared spectroscopy (FTIR), X-ray diffractometer (XRD) and scanning electron microscopy (SEM). SEM images revealed the formation of a more porous membrane structure and smoother surface. The electrochemical and physical properties of CEMs were characterized comprising water content, contact angle, ion exchange capacity (IEC) and thermal stability. Membrane water content, surface hydrophilicity and IEC were enhanced with increase of DS and NPHCs blend ratios in casting solution. Furthermore, the diffusion coefficient was also improved slightly with increase of DS and NPHCs blend ratios in prepared membranes. Membrane potential, permselectivity, transport number and areal membrane resistance all showed decreasing trends by the increase in NPHCs blend ratio in casting solution. These results indicated that the prepared membrane has good prospective and great potential for desalination in electrodialysis applications.

Keywords: Ion Exchange Membrane, Porous Structure, Homogeneous, Electrodialysis, Desalination

INTRODUCTION

Ion exchange membranes (IEMs) are widely studied and employed as active separators in diverse electro-driven processes. In this kind of membrane, ion-functionalized groups attached to polymer backbone will dissociate after the permeation of sufficient water molecules, releasing cations or anions for the transfer of corresponding ions under the influence of an electrical potential difference [1]. IEMs are efficient tools in industrial fields including water purification, food processing and many more processes [1-5].

Particularly, for desalination and ionic separation, IEMs should have high ionic conductivity and permselectivity as well as good thermal, chemical and mechanical stability, and high cost-effectiveness [6-13]. To achieve these properties, selection of preparation methods, different polymeric matrix, variation of functional groups and use of various additives are utilized as strategic tools. Among them, blend method for membrane modification is simple and easy to operate, and this method is a technique to improve the electrical and physical properties of homopolymers [4-6]. Simultaneously, preparing porous ion exchange membranes may be a vital step in these applications [1,21,33].

High performance polymers with polyaryl skeletons such as polyarylsulfone, polyphenylsulfide and poly(ether ether) ketone have been largely designed as alternative materials to IEMs [14-17]. Among these high performance polymers, polyethersulfone (PES) has been regarded as a desirable polymer matrix candidate for membrane formation due to its good flexibility, mechanically stable and low cost [7,18]. However, this polymer is a hydrophobic material and consequently does not dissolve in conventional dipolar solvents, which restricts its application. To improve solubility in dipolar solvents, PES was modified by various electrophilic substitutions. Among the PES derivatives, aryl substituted sulfonated PES (SPES) is a desired polymer which has been employed as a membrane material for gas separation, reverse osmosis, ultrafiltration, and cation exchange membranes. Mabrouk et al. studied the effect of SPES on electrochemical applications [19], but these membranes have a dense membrane structure that affects membrane properties [21]. In recent years, polymer blending membranes have produced significant results in electrodialysis. Amado et al. synthesized polystyrene/polyaniline composite membranes and obtained a better performance membrane with good zinc ion transport capacity [20]. In porous membrane research, Klaysom et al. exploited SPES

†To whom correspondence should be addressed.
E-mail: mzyxy199@163.com, gxl_ouc@126.com

as a membrane matrix to prepare the surface functionalized mesoporous silica porous ion exchange membrane, which enhanced ionic conductivity of the membrane [21]. However, the preparation process of these mesoporous silica membrane materials is cumbersome and sophisticated, so looking for a membrane material with simple preparation method is a problem to be solved in this study.

Chitosan (CS), a cost-effective and eco-friendly polymer from the exoskeleton of crustaceans such as crabs and shrimps and from the cell walls of fungi, has been used as membrane material for the preparation of ion exchange membrane due to its excellent biocompatibility, biodegradability, non-toxicity, chemical and thermal stability [22-24]. CS is a cyclo-aliphatic polymer that contains certain functional groups--amino groups (-NH_2) and hydroxyl groups (-OH) that can provide CS with high hydrophilicity [25-28]. Moreover, these functional groups allow chemical modification to improve the properties of chitosan membrane. However, since there are no mobile hydroxyl ions in its structure, the pristine CS membrane shows much lower ionic conductivity, which limits the application of the material in various fields [24]. To improve the performance of chitosan membrane, chemical modification was employed to modify the chitosan properties for preparing composite membranes with better hydrophilicity, surface charge and biological compatibility by many researchers [29,30]. Nevertheless, there are very limited works investigating the use of CS for membrane design, especially porous IEMs suitable for various applications such as electrodialysis, fuel cell, desalination and water purification [31-33].

The objective of this work was to prepare homogeneous ion exchange membranes with controllable porosities and structures by blending SPES and NPHCs. The simplicity of the blending technique allows the membrane to be cost-effective, provides the potential for combining the attractive features of each blend component while at the same time reducing their deficient characteristics. The effects of DS and NPHCs content on physicochemical, morphological and ion exchange properties of the prepared membranes have been evaluated. The structural composition, morphologies and thermal stability were characterized by Fourier transform infrared spectroscopy (FT-IR), X-ray diffractometer (XRD), scanning electron microscopy (SEM), differential scanning calorimetry (DSC); and the basic membrane properties such as water content, contact angle, ion exchange capacity (IEC) and diffusion potential of NaCl were investigated by chemical and electrical methods. The results are valuable for further studies on the use of chitosan to improve the dense structure of IEMs.

EXPERIMENTAL

1. Materials

Chitosan (80-95% degree of deacetylation) was purchased from Sinopharm Chemical Reagent Company Ltd., China. Polyethersulfone (PES, molecular weight is about 50000) flakes (ULTRASON® E 6020 P, BASF) were dried 24 h at 80 °C in a vacuum before the reaction. Phthalic anhydride (99.7%) (Bodi, Tianjin), Dichloromethane (Fuyu, Tianjin), N,N-dimethylformamide (DMF) (Bodi, Tianjin) and N-methylpyrrolidone (NMP) (Kermel, Tianjin) were of analytical reagent. Chlorosulfonic acid and G4 sand filters were provided by Qingdao Jingke Chemicals Co. (Shangdong, China). All other chemicals were of analytical reagent by Chengdu Keshi Co. (Chengdu, Sichuan).

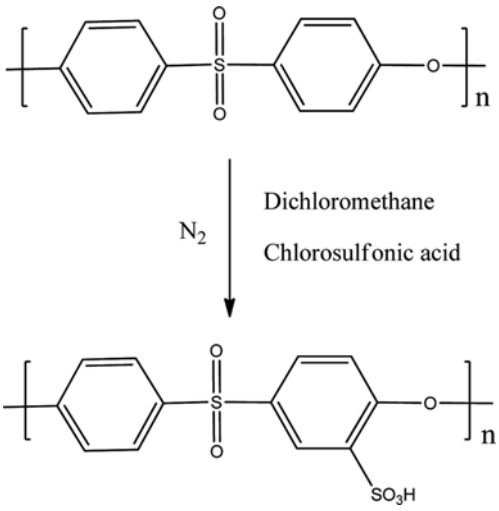

Scheme 1. Schematic representation of sulfonation of polyethersulfone.

2. Sulfonated Polyethersulfone Preparation

Polyethersulfone (PES) was sulfonated according to the procedure reported in the literature [33]. The synthetic path is presented in Scheme 1. Briefly, 4 g of PES was added to 50 g of dichloromethane in a three-necked reaction flask under N_2 atmosphere, and dissolved by stirring at room temperature to form homogeneous solution. 5-10 mL of chlorosulfonic acid was transferred into a constant pressure funnel, and then gradually and slowly added to the solution at a period of time. After a determined stirred time, the mixture was precipitated into cold water under agitation, and the products were recovered by filtration and washed with deionized water until pH was approximately 6-7. Finally, the sulfonated polyethersulfone (SPES) was dried under vacuum at 60 °C for two days.

Degree of sulfonation (DS) is the fraction of the sulfonated monomer units after the reaction. It was determined as follows [34]. First, 0.3 g of SPES was stirred in 30 ml of 2 M NaCl solution for 24 h to release the H^+ ions. Then the mixture was titrated with standardized 0.1 M NaOH solution using phenolphthalein as an indicator. The DS was calculated according to Eq. (1):

$$DS = \frac{0.244(M_{NaOH} \times V_{NaOH})}{W - 0.081(M_{NaOH} \times V_{NaOH})} \times 100\% \quad (1)$$

where M_{NaOH}, V_{NaOH} and W are the concentration of standard NaOH solution, volume of NaOH and weight of dry SPES, respectively. 244 g/mol is the molecular weight of PES repeat unit and 81 is the molar mass of the SO_3H group.

3. N-phthaloyl Chitosan Preparation

N-phthaloyl chitosan (NPHCs) was prepared according to the procedure reported in the literature [32,35]. The synthetic path is presented in Scheme 2. In brief, 1 g chitosan was reacted with 4.48 g phthalic anhydride in 20 ml DMF. The mixture was stirred at 130 °C for 6 h, and then was poured into a large amount of ice-cold water

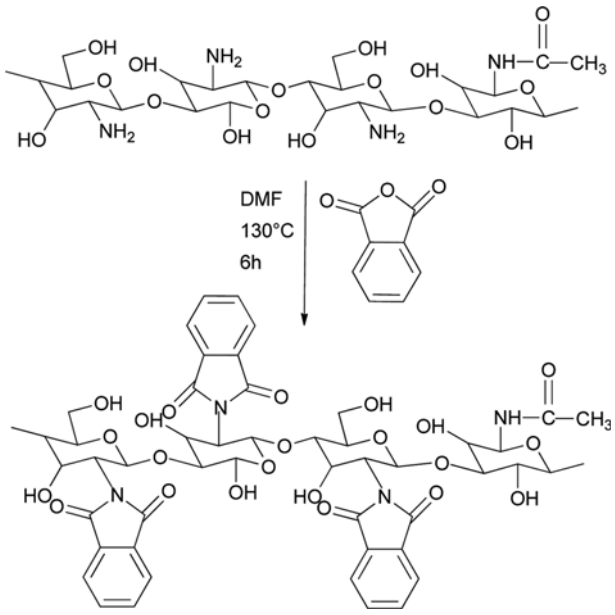

Scheme 2. Schematic representation of the prepared N-phthloyl chitosan.

to give NPHCs. The product was purified by ethanol and ethyl ether; then was dried at 40 °C under vacuum for 24 h.

4. Membrane Preparation

Several ratios of SPES and NPHCs were dissolved in NMP and stirred at 60 °C in a closed flask until a clear solution was obtained, then the stopper was removed and stirring continued for 10 h. The viscous solution was filtered with G4 sand filter immediately and then set for 24 hours. Membrane was prepared by casting viscous solution on a glass plate and spread slowly to form a homogeneous liquid state, before being dried in an oven at 100 °C for 24 hours and then under vacuum at 40 °C for 12 hours. The glass plate was removed and immersed in deionized water to separate the membrane from the glass plate. To discuss the effects of sulfonation degree on the properties of composite membranes, different DS of SPES and NPHCs composite membranes were prepared in the same manner.

5. Polymers and Membrane Characterization

5-1. Morphological and Structural Studies

Morphology of the membranes was observed using scanning electron microscope (Hitachi S4800, Japan). Membrane surface was plated with gold using a sputter coater. The potential was 10 kV and the magnification of 50.0 k. To obtain sharp cross-sectional surface fracture, the samples were cut in liquid nitrogen, then the captured water was dried in an oven at 40 °C overnight.

The functional groups of SPES, NPHCs and composite membranes were analyzed by using FT-IR Spectrometer (Nicolet 380, America). FT-IR scans were taken between 400 and 4,000 cm^{-1} in absorbance mode. The crystalline structure of samples was characterized by the X-ray diffractometer (Utima IV, Japan). XRD experiment was scanned between 5° and 50° at a rate of 8°/min.

5-2. Water Content

Water content was determined by measuring the weight change before and after expansion in the distilled water [16]. The membrane surface was washed with distilled water and then the membrane was dried in a vacuum desiccator for 48 hours, and the weight was W_{dry}. The dried membrane was immersed in distilled water for 48 hours, and then the membrane was removed with absorbent paper to dry the surface moisture, and the weight of W_{wet} was recorded. Water content was obtained from Eq. (2):

$$\text{Water content}\% = \frac{W_{wet} - W_{dry}}{W_{dry}} \times 100\% \quad (2)$$

To reduce the experimental error, each sample was measured three times and their average value was recorded.

5-3. Water Contact Angle Measurements

The contact angle of the membrane surface was measured by measurement apparatus (Krüss DSA100, Germany) according to the fixed droplet method. Briefly, a water droplet (about 3 μL) on a flat dried membrane surface and the image was captured 5 seconds after introducing the droplet. Deionized water was used as the probe liquid in all measurements. At least five angles were measured for each sample and then the average value was calculated and used in this work. All experiments were carried out in the ambient conditions.

5-4. Thermal Stability of Membranes

The thermal properties of the blend membranes were examined by the differential scanning calorimeter (Mettler Toledo DSC 1, Switzerland) in nitrogen atmosphere. 10 mg samples were measured in an Al crucible with a small hole. The samples were heated from 30 °C to 300 °C at a heating rate of 10 °C·min^{-1}.

5-5. Ion Exchange Capacity (IEC) and Fixed Ion Concentration (FIC)

Ion exchange capacity can reflect the concentration of active groups within the membrane, but also reflect its ability to exchange with the anti-ion level. IEC value was determined by titration [36]. Briefly, the membrane was washed repeatedly with 1 M HCl and soaked for 24 hours, and followed by washing with deionized water to remove the H^+ contained in the surface, immersing the membrane in 2 M NaCl for 48 hours. Then the solution was titrated with NaOH using phenolphthalein as an indicator. The IEC value was obtained from Eq. (3):

$$\text{IEC} = \frac{C_{NaOH} \times V_{NaOH}}{W_{dry}} \quad (3)$$

where C_{NaOH} (mol/L) is the concentration of NaOH, V_{NaOH} (mL) refers to the volume of NaOH solution required for neutralization; W_{dry} is the weight of the dry membrane.

The fixed ion concentration (FIC) can be calculated by Eq. (4):

$$\text{FIC} = \frac{\text{IEC}}{\text{Water content}} \quad (4)$$

5-6. Diffusion Coefficient

Diffusion coefficient reflects the ability of the electrolyte to pass through the membrane under the effect of concentration, and has a certain correlation with the membrane porosity. As shown in Fig. S1, blend cation-exchange membranes were fixed in the middle and contacted with circulating NaCl solution (chamber I) and circulating deionized water (chamber II) on both sides. The conductivity of the deionized water was measured and recorded by a

conductivity meter. Use the following formula (5) to calculate the results [37,38].

$$K_s = \frac{D}{t_m} = \frac{v\theta k}{s\Delta C_0} \quad (5)$$

where K_s is permeability coefficient of NaCl; D is diffusion constant of NaCl; t_m is the thickness of membrane; v is volume of NaCl solution; θ is slope of the linear relation between conductivity and concentration at the deionized water side; K is the slope of the linear relation between time and conductivity at the deionized water side; s is the effective membrane area; ΔC_0 is concentration difference across the blend membrane.

5-7. Membrane Electrochemical Properties

5-7-1. Membrane Resistance

The electrical resistance of the membranes was measured by using a hand-made acrylic plastic cell composed of two parts separated by a membrane, as described earlier [39,40]. The prepared membrane was equilibrated in 0.5 M NaCl before being mounted in the cell between platinum electrodes with effective area of 1 cm^2. The resistance of the membrane was measured at room temperature by LCR meter operated at 10 KHz AC (TH2810D, Changzhou Tonghui Electronic Co., Ltd.). The membrane resistance is calculated by using difference resistance between the cell (R_c) and electrolyte solution (R_s) ($R_m = R_c - R_s$).

5-7-2. Membrane Potential and Transport Number

Membrane potential was measured in two compartment cells, in which a vertical membrane of 3.0 cm^2 effective area separated two solutions of 0.5 M NaCl and 1.0 M NaCl, respectively. The experimental setup is shown in Fig. S2. The potential difference across the membrane was measured using a digital multimeter (Victor, model VC890D, China) which was connected to Ag/AgCl reference electrodes. The measurement was repeated until a constant value was obtained. The transport number, t_i^m, was then calculated using the following modified Nernst equation [33]:

$$E_m = (2t_i^m - 1)\frac{RT}{nF}\ln\left(\frac{a_1}{a_2}\right) \quad (6)$$

where t_i^m is the transport number, E_m is the measured potential (V), R is the gas constant, T is the temperature (K), F is the Faraday constant, n is the electrovalence of counter-ion and a_1 and a_2 are solutions electrolyte activities in contact membrane surfaces. The ionic permselectivity of membranes also is quantitatively expressed based on the migration of counterion through the ion-exchange membrane as follows [41].

$$P_s = \frac{t_i^m - t_0}{1 - t_0} \quad (7)$$

where t_0 is the transport number of counter ions in the solution phase.

RESULTS AND DISCUSSION

1. Membrane Structure--chemistry

IR spectroscopy was used for the qualitative analysis; by identifying specific absorption peaks for particular groups, the chemical nature of materials such as chemical bonds can be evaluated. Hence each substance was analyzed by using FT-IR to determine if the product had been synthesized successfully.

Fig. S3 shows the FT-IR spectrum of PES and SPES; the presence of strong peak at 1,240 cm^{-1} is assigned to the ether C-O-C stretch of the PES moiety and the peak at 1,101 cm^{-1} due to O=S=O stretching. Aromatic C-H bond could be detected at 1,068 cm^{-1}. After the sulfonation process, the bands at 1,026 cm^{-1} and 1,147 cm^{-1} in the SPES spectrum could be assigned to the symmetrical and asymmetrical stretching vibrations of sulfonic groups, respectively [42,43]. Also, the increase in absorption peak at 3,444 cm^{-1} was the result of stretching of the OH (-SO_3H) groups [43].

Fig. S4 presents the FT-IR spectrum of chitosan and NPHCs. Absorption peak at 1,599 cm^{-1} is related to -NH_2 bending vibration, and absorption at 2,885 cm^{-1} is responsible for C-H bond. The broad peaks at 3,469 cm^{-1} are substantially overlapping with chitosan, which is the combined band of O-H in the molecule and the N-H vibrational peak in the amide. 1,780 cm^{-1} is the characteristic peak of NPHCs. Absorption peak at 721 cm^{-1} is the out-of-

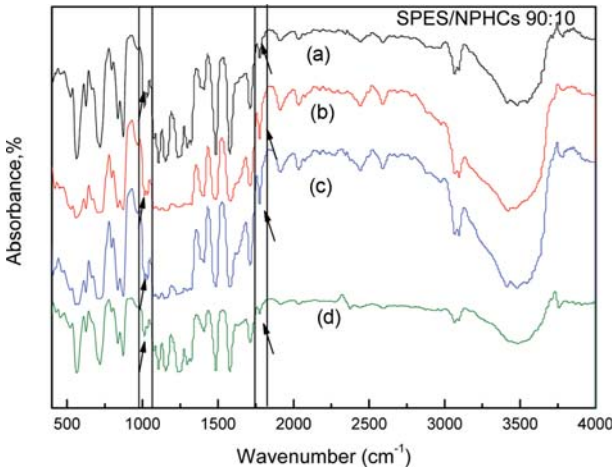

Fig. 1. FT-IR spectra for different DS of SPES/NPHCs blend membranes (at SPES/NPHCs 90 : 10): (a) 15%DS, (b) 20%DS, (c) 25%DS, (d) 30%DS.

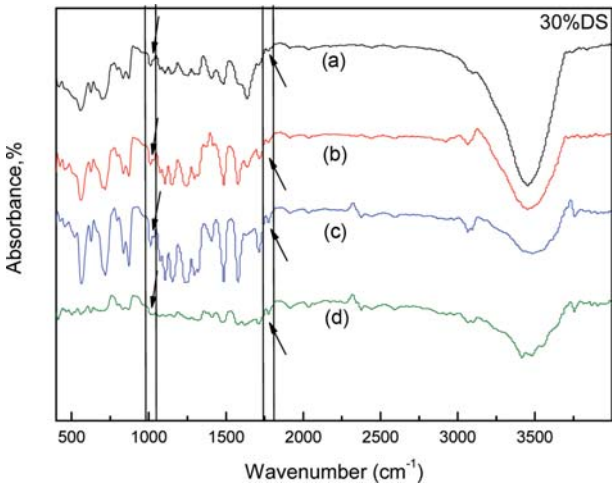

Fig. 2. FT-IR spectra for different ratio of SPES/NPHCs blend membranes (at 30%DS): (a) 80 : 20, (b) 85 : 15, (c) 90 : 10, (d) 95 : 5.

plane bending vibration peak of O-substituted benzene in NPHCs, which confirms the presence of benzene rings and two imide groups in the derivatives. Vibration of C-N bond at 1,390 cm^{-1} was significantly enhanced, indicating that the reaction occurred mainly on the amino group [44].

Fig. 1 and Fig. 2 represent the FT-IR of the different blend membranes. Absorption peak at 1,780 cm^{-1} indicates the presence of NPHCs in the polymeric matrix. Absorption peak at 1,026 cm^{-1} related to sulfonic groups confirms the presence of SPES in the membrane.

XRD patterns were used to determine the change of material crystalline nature. The crystalline nature plays a very important role in understanding the substance's solubility. Therefore, the XRD patterns of each polymer were studied.

Fig. S5 represents the XRD pattern of NPHCs and chitosan. Chitosan shows broad bands at 2θ=20° due to intramolecular and intermolecular hydrogen bonds [45]. The decrease of peak value in NPHCs implies the decrease of crystallinity, which is due to the acylation reaction promoting the destruction of hydrogen bonding involving -NH_2 group. Simultaneously, the obtained NPHCs exhibited affinity for organic solvents consistent with previous results, which makes the foundation for the blending of the two materials [46].

The X-ray diffractograms of the membranes prepared using different DS and SPES/NPHCs in various ratios are shown in Fig. 3 and Fig. 4 respectively. From the XRD patterns of the membranes, the diffraction peaks were shifted at different degrees after the two materials were mixed (SPES shows broad bands at 2θ=20°, not shown in the literature [31]), indicating that there may exist interactions between SPES and NPHCs.

Fig. 3 shows the effect of DS on the crystallinity of the blend membranes. With the increase of DS, the intensity of the crystalline peak value at 2θ=17° decreased due to the hydrophilic group -SO_3H. As presented in Fig. 4, NPHCs content in the blend membrane increases and the strength of the peak value at 2θ=22° decreases, indicating that modified chitosan destroys the rigid structure and makes the polymer transition from crystalline nature to amorphous nature. The crystalline portion of the membrane usually prevents water from entering the membrane; thus the most amorphous membrane is the most promising membrane in the desalination process.

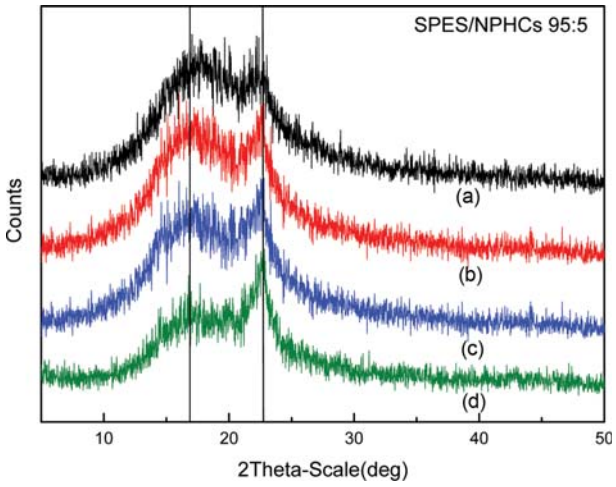

Fig. 3. X-ray diffractogram for different DS of SPES/NPHCs blend membranes (at SPES/NPHCs 95 : 5): (a) 15%DS, (b) 20%DS, (c) 25%DS, (d) 30%DS.

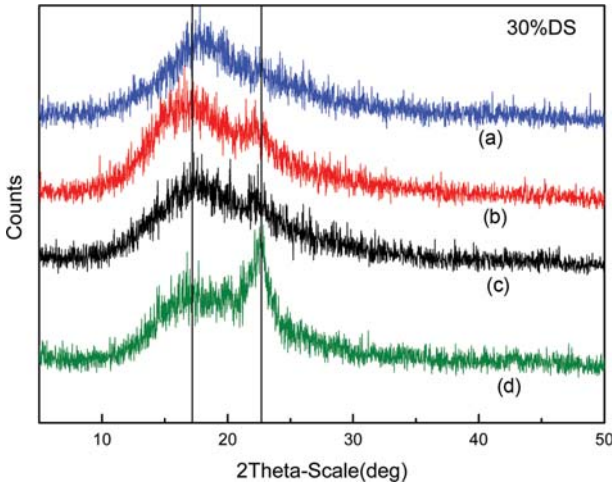

Fig. 4. X-ray diffractogram for different ratio of SPES/NPHCs blend membranes (at 30%DS): (a) 80 : 20, (b) 85 : 15, (c) 90 : 10, (d) 95 : 5.

2. Membrane Structure--thermal Stability

DSC is a commonly used thermal analysis tool that helps to find the glass transition temperature (Tg) and analyzes the thermal stability of the material. Tg of the polymer is an important criterion for the compatibility of polymer components. The completely miscible polymer blend has a single Tg, while the immiscible polymer blend has a plurality of Tg values [47,48].

The DSC curves of blend membranes with different DS and

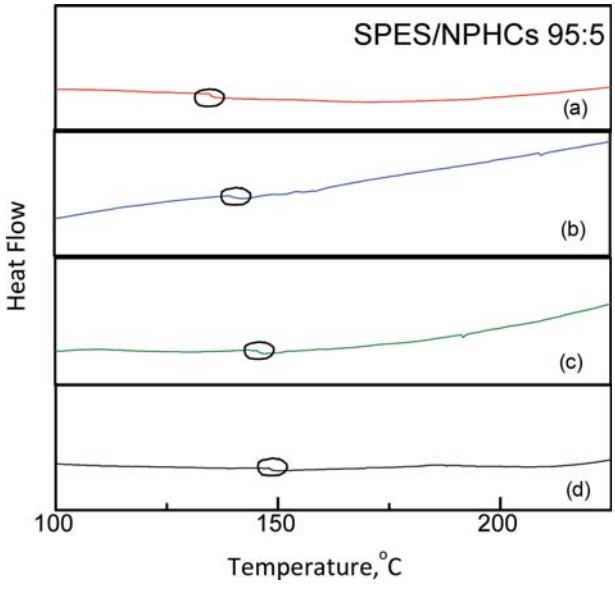

Fig. 5. DSC curves for different DS of SPES/NPHCs blend membranes (at SPES/NPHCs 95 : 5): (a) 15%DS, (b) 20%DS, (c) 25%DS, (d) 30%DS.

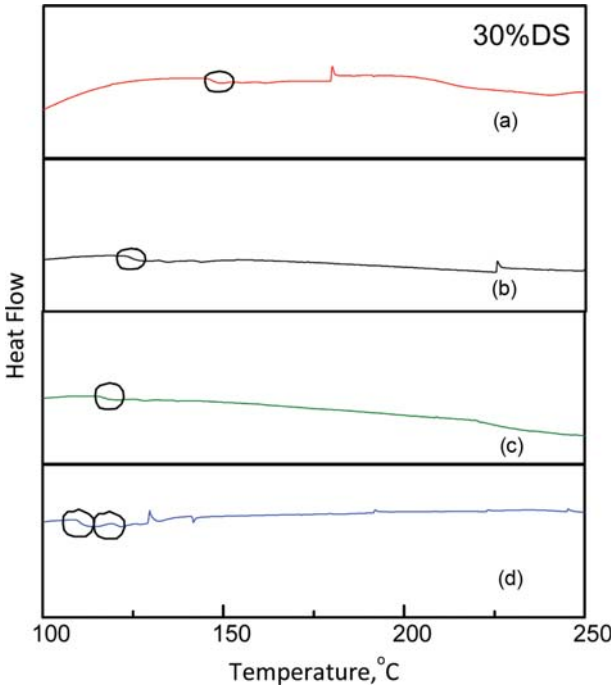

Fig. 6. DSC curves for different ratio of SPES/NPHCs blend membranes (at 30%DS): (a) 80 : 20, (b) 85 : 15, (c) 90 : 10, (d) 95 : 5.

different NPHCs content are shown in Fig. 5 and Fig. 6, respectively. Fig. 5 shows Tg increased with the increasing DS, which was also confirmed by Wang [49]. Moreover, each DSC trace shows a single Tg value, indicating good miscibility between SPES and NPHCs due to the formation of van der Waals interactions. In Fig. 6, with the increase of NPHCs content, the Tg of the blend membrane decreases, which means that the thermal stability of the membrane decreases with the increase of NPHCs content. The difference in Tg values is due to the polymer domain interactions produced by the different forms of various NPHCs content and also to the differences in the mechanical properties of the blend membranes. Moreover, SPES/NPHCs 80 : 20 have two Tg which may be attributed to the presence of ionic cluster [50].

3. Membrane Structure-morphology

The microscopic morphology of the membranes helps to determine the importance of membrane in the mechanism of permeability and selectivity. Thus, the morphology of prepared membranes was evaluated by scanning electron microscopy.

Fig. 7 and Fig. 8 present SEM images of blend membranes with different DS and different NPHCs content, respectively. The surface morphology of membrane showed a uniform and smooth without visible flaws, which indicates that the blend membranes have good compatibility. As shown in Fig. 7, the increase in DS makes the surface go from smooth to rough, while the pore size becomes smaller and the number of pores increases, possibly due to higher DS causing faster coagulation [7]. Similarly in Fig. 8, the increase in the size of pores upon increasing the NPHCs content in the membranes can be observed clearly. Similar results were reported by Kanagaraj et al. [51] At highest loading of NPHCs (80 : 20), the pore size significantly increases due to the additives tending to form clusters (Fig. S6 is the use of Nano Measurer for size distribution analysis; the average value of 80 : 20 is about three-times of 90 : 10), but

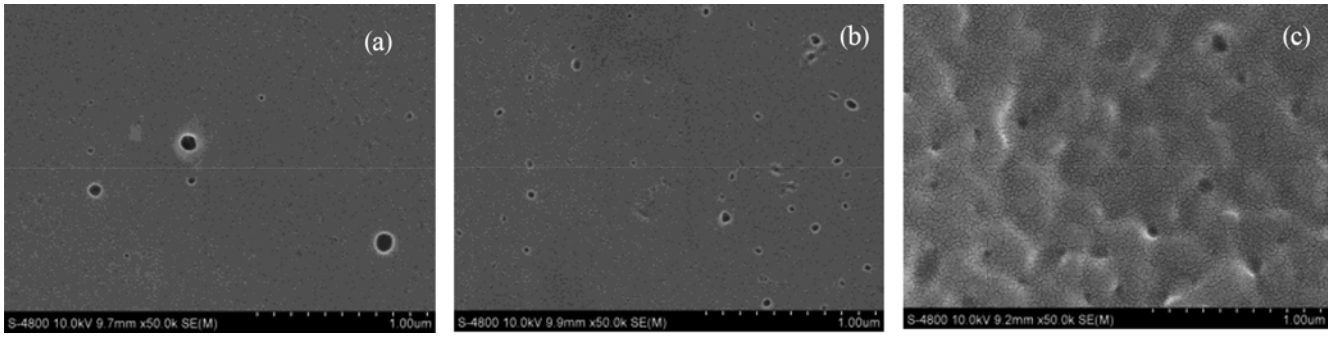

Fig. 7. SEM images for different DS of SPES/NPHCs blend membranes (at SPES/NPHCs 95 : 5): (a) 15%DS, (b) 20%DS, (c) 30%DS.

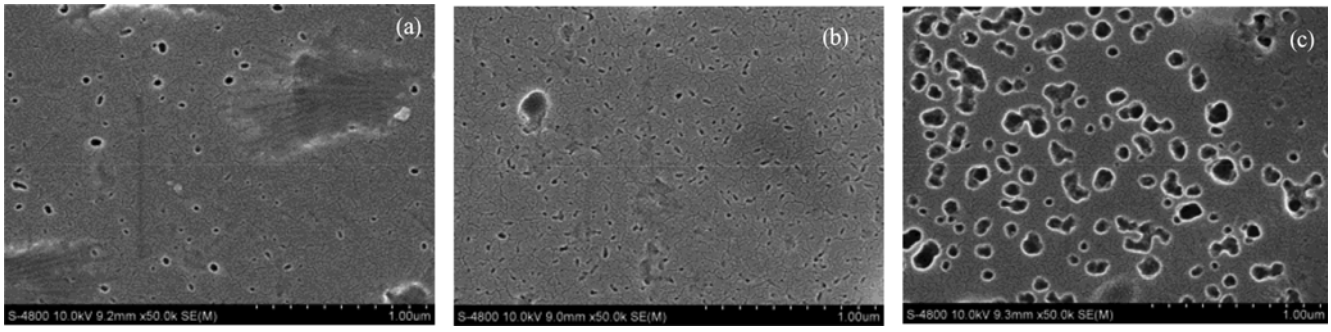

Fig. 8. SEM images for different ratio of SPES/NPHCs blend membranes (at 30%DS): (a) 90 : 10, (b) 85 : 15, (c) 80 : 20.

Table 1. The physical properties of membranes with different DS (at SPES : NPHCs 90 : 10)

Membrane	Water content%	IEC ($mM \cdot g^{-1}$)	Contact angle (°)	FIC
SPES(15%DS) : NPHCs	9.10%	0.48	79.65±2	5.27
SPES(20%DS) : NPHCs	11.35%	0.62	75.51±2	5.46
SPES(25%DS) : NPHCs	13.64%	0.72	73.99±2	5.28
SPES(30%DS) : NPHCs	15.38%	0.81	72.98±2	5.26

Table 2. The physical properties of membranes with different ratio of SPES/NPHCs (at 30%DS)

Membrane	Water content%	IEC ($mM \cdot g^{-1}$)	Contact angle (°)	FIC
SPES : NPHCs 95 : 5	10.34%	0.54	78.54±2	5.22
SPES : NPHCs 90 : 10	15.38%	0.81	72.98±2	5.27
SPES : NPHCs 85 : 15	21.83%	1.16	68.38±2	5.31
SPES : NPHCs 80 : 20	33.33%	1.43	64.67±2	4.29

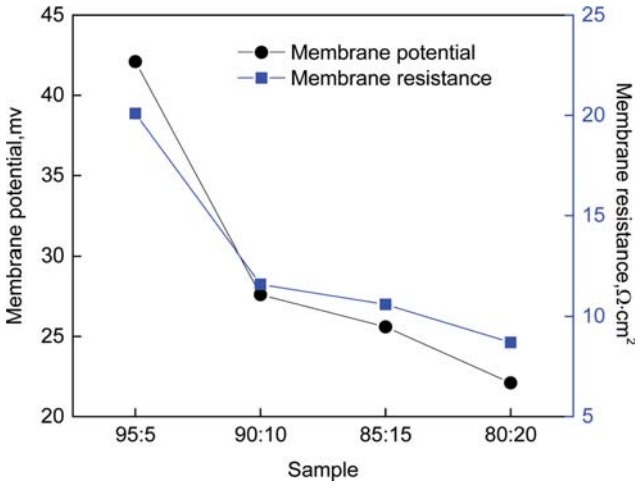

Fig. 9. The effect of blend ratio of SPES to NPHCs in the casting solution on membrane potential and membrane resistance of prepared membranes (at 30%DS).

the distribution of these is still relatively uniform. Under the premise of ensuring the mechanical strength and thermal stability of the membrane, the porous ion exchange membrane has significant effect on the diffusion behavior and exhibits excellent performance in the electrodialysis process [21].

4. Water Content and Ion-exchange Capacity (IEC)

A large number of hydrophilic functional groups in the ion exchange membrane adsorb water molecules. Water molecules act as ion transport carriers, which directly affects the membrane separation performance. Hence, it is important to select membranes with the appropriate water content. Water content increases from lower to higher sulfonation degree (from 15% to 30%, Table 1) due to more hydrophilic sulfonic acid groups in the membrane. NPHCs as a chitosan derivative contains polar functional groups like hydroxyl, and ether groups can improve water content. In Table 2, with the introduction of NPHCs, the water attracting capacity of membrane increases.

The data in the table indicate that water content is proportional to the IEC. Likewise, NPHCs and sulfonation degree all affect the membrane ion exchange performance. Sulfonic acid groups and NPHCs provide active sites for proper interaction between ions and the membrane surface, thereby enhancing the feasibility of ion exchange [52].

5. Fixed Ion Concentration (FIC)

Membrane efficiency is affected by IEC and water content. High IEC and water content can effectively reduce the membrane resistance, but also can cause excessive swelling of the membrane to reduce its ion selectivity and mechanical strength. So the membrane needs to have the appropriate IEC and water content. One important indicator of the synergistic effect of these two parameters is the membrane fixed ion concentration (FIC). Table 1 shows the effect of DS on FIC of the prepared membranes. When the DS of SPES is 20%, the FIC value is 5.46 due to relatively high IEC and suitable water content. Table 2 shows the effect of NPHCs content on FIC of the prepared membranes. As the amount of NPHCs increases, the FIC value decreases due to the swelling of the functional groups [53]. FIC value increased first and then decreased with the increase of NPHCs content. At SPES : NPHCs 85 : 15, the membrane exhibited a suitable FIC compared to the others. The high fixed ion concentration can have better control the pathways of counter ions traffic in the matrix of membrane and, therefore, increases the ionic selectivity.

6. Membrane Potential, Transport Number and Permselectivity

The membrane potential and membrane resistance of prepared membrane are represented in Fig. 9. The membrane potential dropped off by the increase in NPHCs blend ratio in prepared membranes. This can be attributed to the decrease of membrane fixed ionic concentration and also membrane surface charge density. The decrease in Donnan contribution towards total potential developed across the membrane is responsible for the decrease in membrane potential [54]. Moreover, the membrane resistance is practically important due to its relation with energy consumption

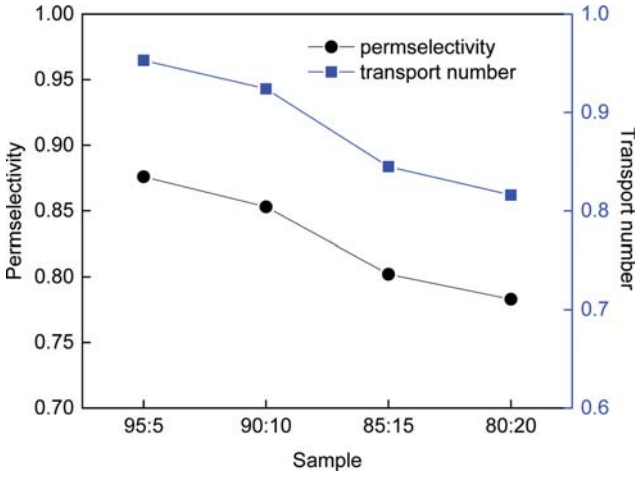

Fig. 10. The permselectivity and transport number of prepared cation exchange membranes with different blend ratio of SPES : NPHCs (at 30% DS).

in the process. The membrane resistance declined with increasing of NPHCs blend ratio in casting solution (Fig. 9). This could be ascribed to the increase in the ion exchange functional groups and an increase in the suitable ion conducting pathways throughout the membrane matrixes. This makes wide ionic transfer channels in membrane matrix and improves the ions transportation, and so reduces the areal electrical resistance [39,40,54].

Both transport number and permselectivity of the prepared membranes are depicted in Fig. 10. It is evidenced that the transport number and the permselectivity of the membrane tended to decrease with increase of NPHCs blend ratio of the casting solution This result can be explained with respect to the decrease in ionic concentration, which facilitates the co-ion percolation through the membrane matrix and so reduces the selectivity and transport number. In addition, the increases of membrane water content and IEC with increase of NPHCs blend ratio in prepared membranes (due to the NPHCs hydrophilic characteristic) makes wide ionic transfer pathways in membrane matrix and reduces the ionic sites domination on ion traffic. This reduces the membrane selectivity and transport number [41,54].

7. Membrane Hydrophilicity

Contact angle is used to characterize the outermost changes in membrane modification to evaluate the hydrophilicity of the membrane. The contact angle data of different DS and different NPHCs content are reflected in Table 1 and Table 2, respectively. In Table 1 the contact angle decreases as the DS increases, indicating the increase in hydrophilicity of the blend membrane [55]. This can be ascribed to the hydrophilic SO_3H polar groups. NPHCs in the blend membrane can increase the hydrophilicity of the membrane observed from Table 2. The value increases with the increase of NPHCs content. The presence of polar carbonyl (OH) groups in NPHCs leads to membrane with higher surface hydrophilicity. Similar results were reported for polysulfone/N-phthaloyl chitosan composite membranes by Padaki et al. [32].

8. Membrane Porosity

As mentioned [21], porous ion exchange membranes have good

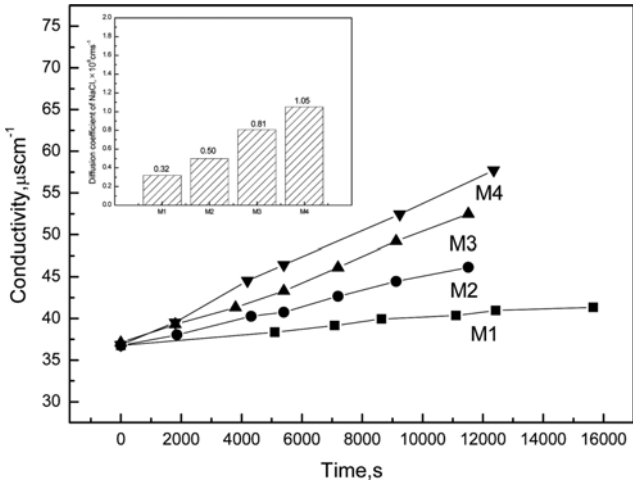

Fig. 11. The effect of DS on NaCl diffusion behavior of prepared ion exchange membranes (at SPES/NPHCs 95 : 5): M1, 15%DS; M2, 20%DS; M3, 25%DS; M4, 30%DS.

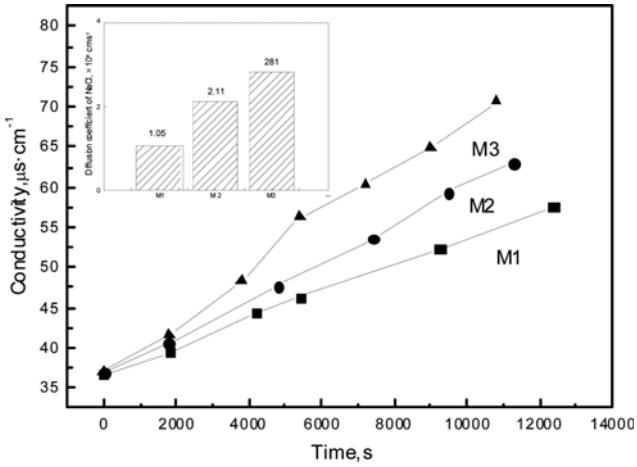

Fig. 12. The effect of NPHCs content on NaCl diffusion behavior of prepared ion exchange membranes (at 30%DS): M1, SPES/NPHCs 95 : 5; M2, SPES/NPHCs 90 : 10; M3, SPES/NPHCs 85 : 15.

properties. The diffusion effect depends on the presence of active ion exchange groups and pores in the membrane. Therefore, to investigate the change in porosity of the prepared membranes under different reaction conditions, the diffusion coefficient was measured [56,57].

As seen in Fig. 11, the NaCl diffusion behavior increased with the increase of DS, especially for M4, a large number of hydrophilic groups (sulfonic acid groups) on the membrane surface contribute to the transport of the electrolyte through the membrane. In Fig. 12, the permeability coefficients of ion through the cation exchange membrane with more NPHCs content were reported to increase, which means that the porosity of the composite membranes increased by the effect of NPHCs. The increase in NPHCs content makes the membrane porosity to accumulate more electrolyte ions and the diffusion of Na^+ is strengthened, which is consistent with above-mentioned IEC experiments. As the NPHCs content increases, the mechanical properties of the membrane are reduced, so the diffusion coefficient of the membrane 80 : 20 is not measured. The membrane M3 was facilitated when compared with that of membrane in the literature [37], this study has gained more satisfactory results.

CONCLUSIONS

Homogeneous ion exchange membranes by blending SPES and NPHCs with controllable porosity and improvement of hydrophilic were successfully prepared. The characterization of membranes by FTIR, XRD and DSC reveals successful reaction and good compatibility between SPES and NPHCs. The porous and smooth morphology of fabricated membranes was confirmed by SEM and diffusion coefficient. The electrochemical and physical properties of blend membrane were affected by the sulfonation degree of the SPES and the content of NPCHs. Based on the results, the optimized blending ratio of membrane and sulfonation degree of the SPES should be 85 : 15 (SPES : NPHCs) and 30%, respectively. In addition, high DS and appropriate NPHCs content indeed improve

hydrophilic and porosity of membrane. Membrane potential, permselectivity, transport number and membrane resistance all dropped off with the increase of NPHCs blend ratio in home-made membrane. Although the molecular weight of chitosan, chitosan deacetylation and many other factors will interfere with membrane performance, this work also provides some illumination for the preparation of porous ion-exchange membrane for the electrodialysis process.

ACKNOWLEDGEMENTS

Financial support by the Key Research Project of Shandong Province (NO. 2017CXGC1004), Young Taishan Scholars Program of Shandong Province and Scientific Research Foundation for the Returned Overseas Chinese Scholars, State Education Ministry is gratefully acknowledged.

SUPPORTING INFORMATION

Additional information as noted in the text. This information is available via the Internet at http://www.springer.com/chemistry/journal/11814.

REFERENCES

1. J. Ran, L. Wu, Y. He, Z. Yang, Y. Wang, C. Jiang, L. Ge, E. Bakangura and T. Xu, *J. Membr. Sci.*, **522**, 267 (2017).
2. C. Vogel and J. Meier-Haack, *Desalination*, **342**, 156 (2014).
3. K. H. Choi and T. Y. Jeoung, *Korean J. Chem. Eng.*, **19**, 107 (2002).
4. R. W. Baker, *Membrane Technology and Applications*, 2nd Ed. England, Wiley (2004).
5. S. Hosseini, A. Hamidi, A. Moghadassi, F. Parvizian and S. S. Madaeni, *Korean J. Chem. Eng.*, **32**, 1827 (2015).
6. J. Schauer and L. Brozova, *J. Membr. Sci.*, **250**, 151 (2005).
7. M. Ghasemi, W. R. W. Daud, J. Alam, H. Ilbeygi, M. Sedighi, A. F. Ismail, M. H. Yazdi and S. A. Aljlil, *Energy*, **96**, 303 (2016).
8. T. Chakrabarty, A. M. Rajesh, A. Jasti, A. K. Thakur, A. K. Singh, S. Prakash, V. Kulshrestha and V. K. Shahi, *Desalination*, **282**, 2 (2011).
9. M. Zarrinkhameh, A. Zendehnam and S. M. Hosseini, *Korean J. Chem. Eng.*, **31**, 1187 (2014).
10. M. Reig, H. Farrokhzad, B. Van der Bruggen, O. Gibert and J. Luis Cortina, *Desalination*, **375**, 1 (2015).
11. H. Farrokhzad, S. Darvishmanesh, G. Genduso, T. Van Gerven and B. Van der Bruggen, *Electrochim. Acta*, **158**, 64 (2015).
12. F. Q. Mir and A. Shukla, *Desalination*, **372**, 1 (2015).
13. E. Y. Choi and S. H. Moon, *Desalination*, *Korean J. Chem. Eng.*, **25**, 1151 (2008).
14. T. Chakrabarty, A. M. Rajesh, A. Jasti, A. K. Thakur, A. K. Singh, S. Prakash, V. Kulshrestha and V. K. Shahi, *Desalination*, **282**, 2 (2011).
15. Y. Li, X. Zhang, G. He and F. Zhang, *Int. J. Hydrogen Energy*, **42**, 2360 (2016).
16. H. J. Cassady, E. C. Cimino, M. Kumar and M. A. Hickner, *J. Membr. Sci.*, **508**, 146 (2016).
17. L. Lei, X. Zhu, J. Xu, H. Qian, Z. Zou and H. Yang, *J. Power Sources*, **350**, 41 (2017).
18. A. Saleem, L. Frormann and A. Iqbal, *Polym. Compos.*, **28**, 785 (2007).
19. W. Mabrouk, L. Ogier, S. Vidal, C. Sollogoub and J. F. Fauvarque, *J. Membr. Sci.*, **452**, 263 (2014).
20. F. D. R. Amado, E. Gondran, J. Z. Ferreira, M. A. S. Rodrigues and C. A. Ferreira, *J. Membr. Sci.*, **234**, 139 (2004).
21. C. Klaysom, R. Marschall, S. Moon, B. P. Ladewig, G. Q. M. Lu and L. Wang, *J. Mater. Chem.*, **21**, 7401 (2011).
22. J. Ma and Y. Sahai, *Carbohydr. Polym.*, **92**, 955 (2013).
23. Y. Mansourpanah, A. Kakanejadifard, F. G. Dehrizi, M. Tabatabaei and H. S. Afarani, *Korean J. Chem. Eng.*, **32**, 149 (2015).
24. P. Srinophakun, A. Thanapimmetha, S. Plangsri, S. Vetchayakunchai and M. Saisriyoot, *J. Clean Prod.*, **142**, 1274 (2017).
25. P. Mukoma, B. R. Jooste and H. C. M. Vosloo, *J. Power Sources*, **136**, 16 (2004).
26. R. Kumar, A. M. Isloor and A. F. Ismail, *Desalination*, **350**, 102 (2014).
27. S. S. Shenvi, S. A. Rashid, A. F. Ismail, M. A. Kassim and A. M. Isloor, *Desalination*, **315**, 135 (2013).
28. H. S. Tsai and Y. Z. Wang, *Polym. Bull.*, **60**, 103 (2008).
29. N. Yuana, R. Tsaia, M. Hob, D. Wanga, J. Laic and H. Hsieha, *Desalination*, **234**, 166 (2008).
30. V. Tangpasuthadol, N. Pongchaisirikul and V. P. Hoven, *Carbohydr. Res.*, **338**, 937 (2003).
31. A. Muthumeenal, S. Neelakandan, P. Kanagaraj and A. Nagendran, *Renew. Energy*, **86**, 922 (2016).
32. M. Padaki, A. M. Isloor and P. Wanichapichart, *Desalination*, **279**, 409 (2011).
33. C. Klaysom, S. Moon, B. P. Ladewig, G. Q. M. Lu and L. Wang, *J. Membr. Sci.*, **371**, 37 (2011).
34. C. Klaysom, B. P. Ladewig, G. Q. M. Lu and L. Wang, *J. Membr. Sci.*, **368**, 48 (2011).
35. R. Yoksan and S. Chirachanchai, *Bioorg. Med. Chem.*, **16**, 2687 (2008).
36. M. Zhou, X. Chen, J. Pan, S. Yang, B. Han, L. Xue, J. Shen, C. Gao and B. V. Bruggen, *Desalination*, **415**, 29 (2017).
37. H. L. Yeager and A. Steck, *J. Electrochem. Soc.*, **128**, 1880 (1981).
38. M. Wang, Y. Jia, T. Yao and K. Wang, *J. Membr. Sci.*, **442**, 39 (2013).
39. S. M. Hosseini, S. S. Madaeni and A. R. Khodabakhshi, *Sep. Sci. Technol.*, **46**, 794 (2011).
40. S. M. Hosseini, S. S. Madaeni, A. R. Heidari and A. Amirimehr, *Desalination*, **284**, 191 (2012).
41. G. S. Gohil, V. V. Binsu and V. K. Shahi, *J. Membr. Sci.*, **280**, 210 (2006).
42. W. Zhao, Q. Mou, X. Zhang, J. Shi, S. Sun and C. Zhao, *Eur. Polym. J.*, **49**, 738 (2013).
43. S. Sahebi, S. Phuntsho, Y. C. Woo, M. J. Park, L. D. Tijing, S. Hong and H. K. Shon, *Desalination*, **389**, 129 (2016).
44. A. Zhu, T. Chen, L. Yuan, H. Wu and P. Lu, *Carbohydr. Polym.*, **66**, 274 (2006).
45. R. J. Samuels, *J. Polym. Sci., Part B: Polym. Phys.*, **19**, 1081 (1981).
46. K. Kurita, H. Ikeda, M. Shimojoh and M. Harata, *Biomacromolecules*, **3**, 1 (2002).
47. A. Behboudi, Y. Jafarzadeh and R. Yegani, *J. Membr. Sci.*, **534**, 18 (2017).
48. Q. F. Alsalhy, *Desalination*, **294**, 44 (2012).
49. F. Wang, M. Hickner, Y. S. Kima, T. A. Zawodzinski and J. E.

McGratha, *J. Membr. Sci.*, **197**, 231 (2002).
50. E. B. Orler, D. J. Yontz and R. B. Moore, *Macromolecules*, **26**, 5157 (1993).
51. P. Kanagaraj, A. Nagendran, D. Rana, T. Matsuura, S. Neelakandan, T. Karthikkumar and A. Muthumeenal, *Appl. Surf. Sci.*, **329**, 165 (2015).
52. F. Heidary, A. R. Khodabakhshi and A. N. Kharat, *Korean J. Chem. Eng.*, **33**, 1380 (2016).
53. B. Tong, Md. M. Hossain, Z. Yang, C. Cheng, Y. Wang, C. Jiang and T. Xu, *J. Taiwan Inst. Chem. E.*, **67**, 435 (2016).
54. S. M. Hosseini, A. Gholami, S. S. Madaeni, A. R. Moghadassi and A. R. Hamidi, *Desalination*, **306**, 51 (2012).
55. R. Guan, H. Zou, D. Lu, C. Gong and Y. Liu, *Eur. Polym. J.*, **41**, 1554 (2005).
56. T. Sata, T. Funakoshi and K. Akai, *Macromolecules*, **29**, 4029 (1996).
57. T. Sata, Y. Ishii, K. Kawamura and K. Matsusaki, *J. Electrochem. Soc.*, **146**, 585 (1999).

Supporting Information

Developing homogeneous ion exchange membranes derived from sulfonated polyethersulfone/N-phthaloyl-chitosan for improved hydrophilic and controllable porosity

Zhixue Li*, Zhun Ma*,†, Yuting Xu*, Xiaomeng Wang*, Yongchao Sun*, Rong Wang*, Jian Wang, Xueli Gao***,†, and Jun Gao***

*College of Chemical and Environmental Engineering, Shandong University of Science and Technology, Qingdao 266590, P. R. China
**The Institute of Seawater Desalination and Multipurpose Utilization, SOA, Tianjin 300192, P. R. China
***Key Laboratory of Marine Chemistry Theory and Technology, Ministry of Education, College of Chemistry and Chemical Engineering, Ocean University of China, Qingdao 266100, P. R. China
(*Received 28 November 2017 • accepted 10 April 2018*)

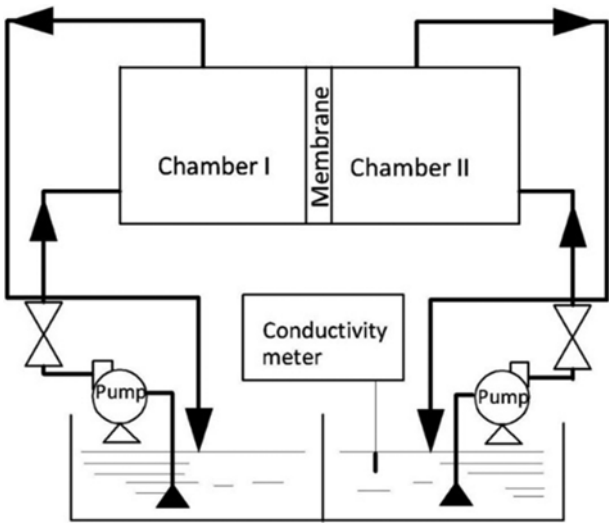

Fig. S1. The setup used for the measurement of diffusion coefficient.

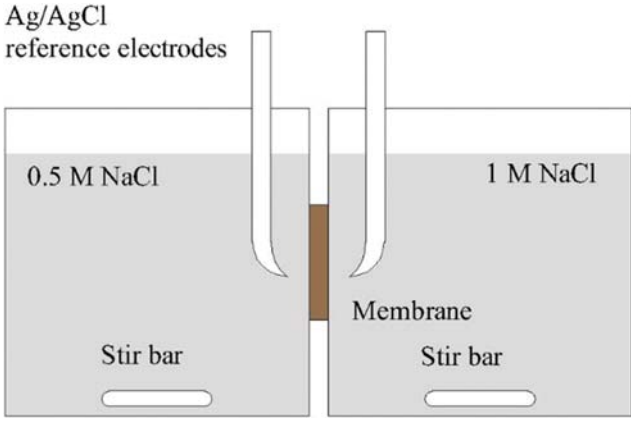

Fig. S2. Schematic of the cell used to measure membrane potential and transport number.

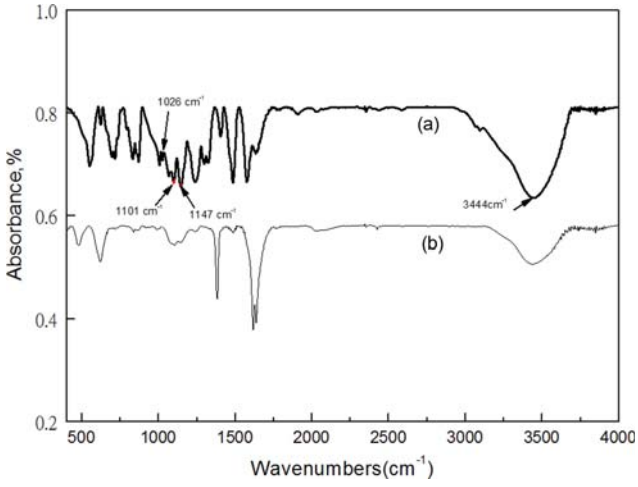

Fig. S3. FTIR spectra for: (a) SPES, (b) PES.

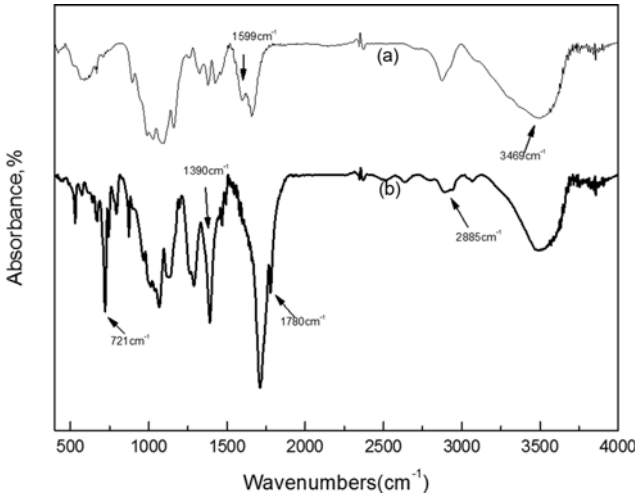

Fig. S4. FTIR spectra for: (a) Chitosan, (b) NPHCs.

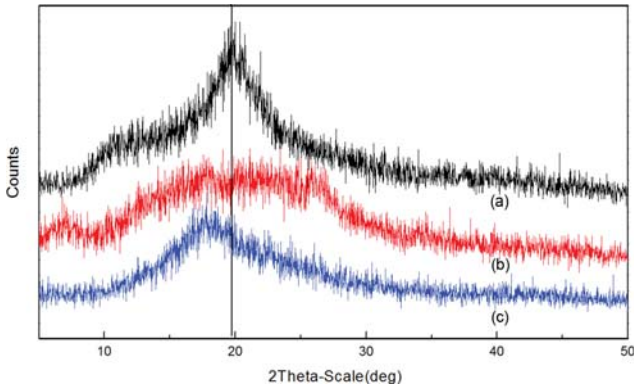

Fig. S5. X-ray diffractogram for: (a) Chitosan, (b) NPHCs, (c) SPES/NPHCs.

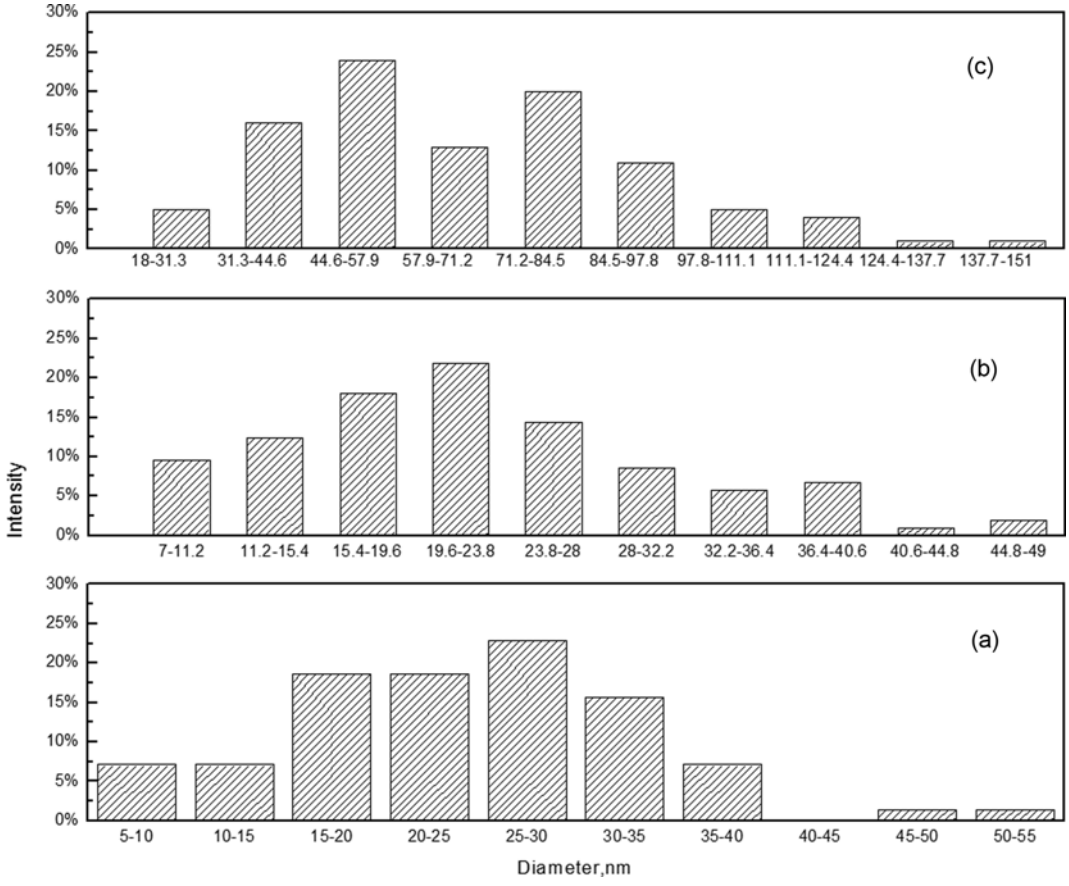

Fig. S6. Size distribution for (a) SPES (30%DS)/NPHCs (90 : 10), (b) SPES (30%DS)/NPHCs (85 : 15), (c) SPES (30%DS)/NPHCs (80 : 20).